Available online at www.sciencedirect.com
ScienceDirect
Palaeogeography, Palaeoclimatology, Palaeoecology 257 (2008) 261–279
PALAEO
www.elsevier.com/locate/palaeo

Last Interglacial fossil elephant trackways dated by OSL/AAR in coastal aeolianites, Still Bay, South Africa

David L. Roberts [a,*], Mark D. Bateman [b], Colin V. Murray-Wallace [c], Andrew S. Carr [d], Peter J. Holmes [e]

[a] *Council for Geoscience, PO Box 572, Bellville 7535, South Africa*
[b] *Sheffield Centre for International Drylands Research, Department of Geography, University of Sheffield, Winter Street, Sheffield, S10 2TN, UK*
[c] *School of Earth and Environmental Sciences, University of Wollongong, NSW 2522, Australia*
[d] *Department of Geography, University of Leicester, University Road Leicester, LE1 7RH UK*
[e] *Department of Geography, University of the Free State, PO Box 339, Bloemfontein 9300, South Africa*

Received 8 January 2007; received in revised form 29 June 2007; accepted 28 August 2007

Abstract

The impressive Pleistocene coastal aeolianite exposures in sea cliffs east of Still Bay on the west–southern coast of South Africa host a rich archive of fossil mammalian trackways, including the African elephant (*Loxodonta africana*). Neither the ichnofossils nor their host sediments have been described in any detail and chronologies remained uncertain. This paper presents a new optically stimulated luminescence (OSL) and amino acid racemisation (AAR) chronology (the first joint application of OSL/AAR dating in South Africa). This provides a temporal framework for assessing the palaeoenvironmental significance of dune sedimentation patterns, pedogenesis and ichnology.

The Pleistocene aeolianite exposures at Still Bay represent the recently eroded remnants of a dune cordon, mainly built by coalesced parabolic dune systems. Sedimentary facies are dominated by large-scale planar cross-stratification formed by foreset progradation in the nose and trailing arms of the dunes and low-angle bedding, chiefly representing sedimentation in low relief interdune terrain. The main dune building wind regime was westerly, associated with cyclonic polar frontal systems (as at the present time). The OSL and AAR dating demonstrate ages ranging from MIS 5e to 5b and termination of Pleistocene aeolian sedimentation at ~90 ka. The Pleistocene aeolianite is separated from the overlying Holocene dunes (dated to ~8 ka), by a major hiatus recorded by a horizon of intense pedogenesis.

Elephant footprints were seen in profile, as casts on the underside of beds and as natural impressions. The taphonomic processes controlling the morphology and preservation of these unique ichnofossils were found to be complex. The presence of *Loxodonta africana* at Still Bay represents the southernmost occurrence of this species recorded to date and possibly, a closer proximity of woodland during MIS 5. This and other observations may indicate a higher moisture regime than at present. There is no available evidence that the elephants were predated by contemporary Middle Stone Age people.

Keywords: Aeolianite; Elephant trackways; Luminescence; Amino acid racemisation; Last Interglacial

* Corresponding author. Tel.: +27 1 948 4754; fax: +27 21 948 8788.
E-mail address: droberts@geoscience.org.za (D.L. Roberts).

0031-0182/$ - see front matter © 2007 Elsevier B.V. All rights reserved.
doi:10.1016/j.palaeo.2007.08.005

1. Introduction

The tectonically stable, trailing edge margin of the southern Cape region of South Africa (Fig. 1) is extensively blanketed by aeolianites, ranging in age from Late Tertiary to Pleistocene and Holocene (Le Roux, 1989; Malan, 1989, 1990). Impressive aeolianite exposures in sea cliffs east of Still Bay are relatively inaccessible and have not previously been described in any detail (Figs. 2 and 3). They contain a rich archive of fossil mammalian trackways (Roberts, 2003) including carnivore, proboscidean (elephant), antelope, equid, rodent as well as reptilian (testudinae). In the context of the new optically stimulated luminescence (OSL) and amino acid racemisation (AAR) chronology presented here, these have the potential to provide further insights into contemporary faunas and therefore, inferences concerning the floras and palaeoenvironments (Roberts, 2003). Only the character and significance of the elephant trackways are considered here; the other traces will be described elsewhere.

Some recent progress has been made in understanding the development and chronology of Quaternary aeolianites along the southern South African coast, particularly through the application of OSL techniques (Bateman et al., 2004; Carr et al., 2006a; Carr et al., 2007; Roberts, in press). However, the available data remain sparse and many available ages are from scattered and typically surficial locations. In the absence of detailed and systematically derived chronologies, reliable correlations and a full understanding of the controls on dune accumulation and preservation and thus, their palaeoenvironmental significance, is still wanting.

Caves eroded into Palaeozoic and Mesozoic rocks along the southern coast during past relative sea level highstands, host a rich archaeological and palaeoenvironmental archive. Of great significance are cave sites such as Die Kelders and Klasies River, which contain the fragmentary remains of some of the earliest known anatomically modern humans (Rightmire and Deacon, 1991; Deacon, 1995; Pearson and Grine, 1997; Deacon and Deacon, 1999). In addition, the well dated Blombos Cave which boasts the oldest purported artwork in the world (~70 ka) is situated only some 20 km west of the study area (Henshilwood et al., 2001, 2002; Jacobs et al., 2003). Thus evidence of human anatomical *and* behavioral modernity, thought to rank among the earliest known, is manifested in the region. One of the key questions therefore, is the degree of interplay between fluctuations in environmental conditions (especially in the flora and fauna) and early human populations. The aims of this paper are, therefore to:

1. Provide a geochronological framework for the Still Bay aeolianites (thus far entirely lacking) via OSL/AAR dating;

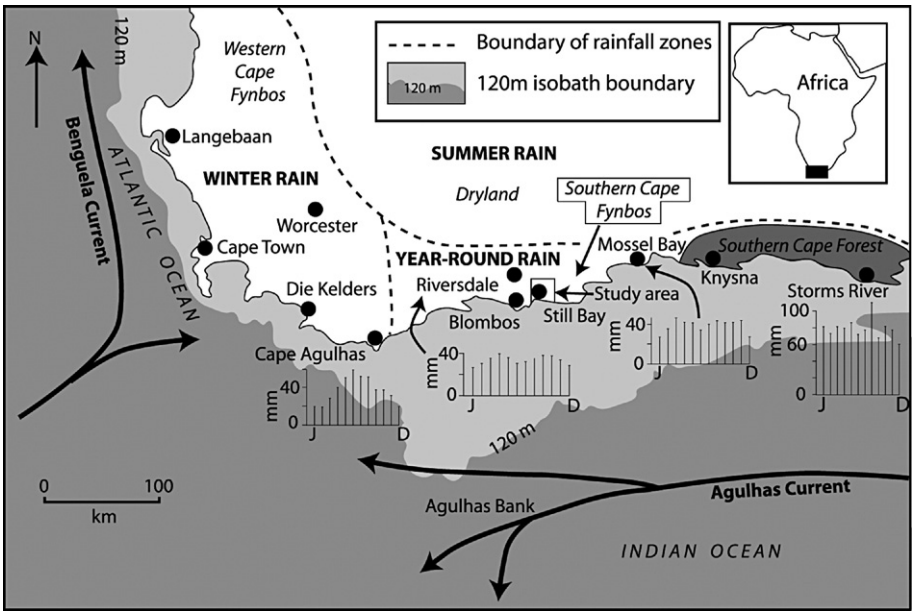

Fig. 1. Locality map of the southern Cape, showing the boundary between the seasonal rainfall regions and vegetation biomes. Also indicated are monthly rainfall patterns (J=January; D=December) along the southern coast based on historical data (South African Weather Bureau, 1986). The 120 m isobath delimits the area exposed during the maximum regression of the Last Glacial (light shading) and highlights the broad shallow shelf off the south coast.

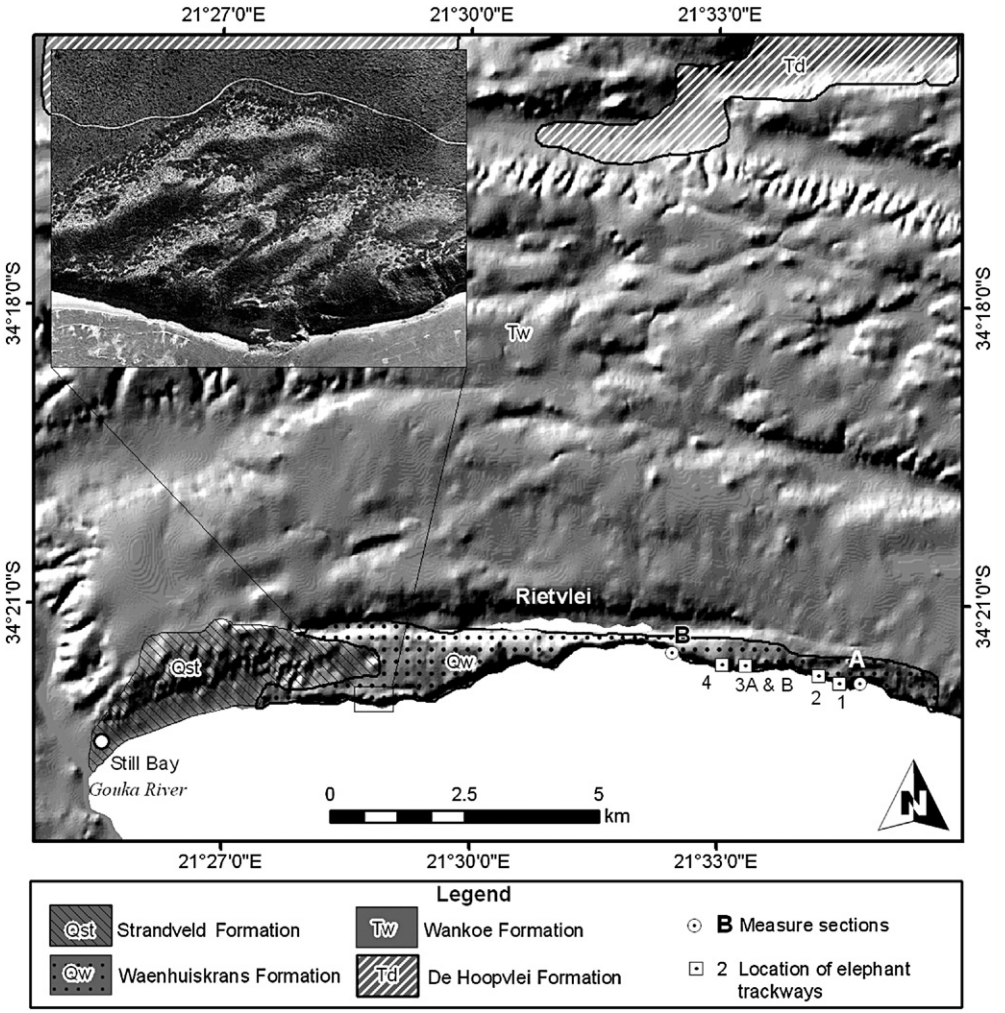

Fig. 2. Geology of the study area and locality of sites mentioned in the text. Inset shows relict Pleistocene parabolic dunes. For explanation of formation names, see Table 1.

2. Analyse aeolian sedimentary facies and pedogenesis at Still Bay to establish their palaeoenvironmental significance and to reconstruct Late Pleistocene landscapes traversed by the elephants;
3. Determine the palaeoenvironmental significance of the presence of elephants and taphonomic aspects of the trackways;
4. Assess the significance of the findings of this study regarding contemporary early modern humans.

In essence, the research focus is to describe, interpret and synthesise various palaeoenvironmentally sensitive features (with emphasis on fossil elephant trackways) of an aeolianite succession in the context a high resolution chronology.

2. Geographic setting and climate

Still Bay lies close to the interface between two major climatic zones. The western region relies almost entirely on (winter) polar frontal, cyclonic weather systems for its rainfall, whereas the eastern zone, including Still Bay derives precipitation from both (winter) cyclonic and (summer) anticyclonic weather systems (Fig. 1), and so experiences a year-round rainfall regime (South African Weather Bureau, 1986). This results in an east–west annual precipitation gradient along the coast with over 1000 mm around Knysna and only ~400 mm in the vicinity of Still Bay (South African Weather Bureau, 1986). The region is therefore, highly sensitive to shifts in the position of

Fig. 3. Site of measured section B in Fig. 4. Low-angle laminated facies of the main elephant trackway horizon (above crouched figures), underlain by negatively weathered protosol (level with crouched figures) and overlain by superposed large-scale foresets. Note the convex upward foresets (middle right), with alternating bundles of darker and lighter laminae.

the intertropical convergence zone and South Atlantic anticylcone, which mediate the relative influence of cyclonic and anticyclonic climatic systems (Tyson, 1999). Westerly winds dominate in the winter and easterlies during the summer (Kruger, 2004) and the mean diurnal temperature is ~17.5 °C.

The study area is also situated near the convergence of the cold Benguela and warm Agulhas oceanographic systems (Fig. 1). Quaternary and recent fluctuations in their relative strength and position have had profound implications for patterns of sea surface temperatures and upwelling systems in the region and hence overall precipitation (Walker, 1990; Cohen and Tyson, 1995). The shallow Agulhas Bank adjacent to the study area would have greatly magnified the effects of Quaternary sea level fluctuations (Fig. 1), repeatedly exposing and flooding great tracts of land (Dingle and Rogers, 1972) and increasing the continentality of presently coastal environments during lowstands (Fig. 1).

Indications exist that floral biomes and faunal ranges have repeatedly expanded and contracted in the region during the Pleistocene in response to the driving forces described above (e.g. Cowling, 1983; Carr et al., 2006b; Irving, 1998), but evidence remains sparse. Still Bay is also close to the interface between two major vegetation biomes, the southern Cape temperate forest and the drier, scrubby *fynbos* (Fig. 1), and potentially may record migration of this interface.

3. Stratigraphy and sedimentation

3.1. Introduction

The region is underlain by Devonian mudrocks (Bokkeveld Group) of the Cape Supergroup. Repeated Cenozoic marine trangressions have bevelled a broad, gently seaward-dipping coastal platform in these susceptible strata (Malan, 1989, 1990) mantled by a veneer of Late Tertiary marine shelly gravels (De Hoopvlei Formation, Table 1) and overlain by variable thicknesses of calcified aeolianite (Wankoe Formation) of similar age (Malan, 1989, 1990). Near Still Bay, the Wankoe Formation forms a shoreline-parallel series of dune cordons (Fig. 2).

Table 1
Lithostratigraphy of coastal Cenozoic sediments of the west–southern coast (Malan, 1990)

Bredasdorp group			
Formation	Age	Lithology	Genesis
Strandveld	Holocene	Calcareous sands	Eolian
Waenhuiskrans	Middle to Late Pleistocene	Calcarenites	Eolian
Klein Brak	Middle to Late Pleistocene	Shelly sands and gravels	Shallow marine
Wankoe	Late Tertiary	Calcarenites	Eolian
De Hoopvlei	Late Tertiary	Shelly sands and gravels	Shallow marine

The aeolian sedimentary patterns established in the Late Tertiary persisted into the Quaternary. Nearer the coast, younger Middle to Late Pleistocene dune cordons (Waenhuiskrans Formation) and active Holocene dune-fields (Strandveld Formation), form a seaward younging succession (Fig. 2; Table 1). East of Still Bay, rapid erosion of the seaward-most Pleistocene dune cordon in this regime of high wave energy has formed spectacular three dimensional exposures of calcified aeolianites in steep sea cliffs along a coastal stretch of some 12 km (Figs. 2 and 3). The cordon is separated from an older, much larger counterpart by a narrow interdune slack, occupied by an elongate freshwater lake (Rietvlei) about 6 km east of Still Bay (Fig. 2). The sea cliffs range up to 70 m in height with a scree of fallen calcarenite blocks and sand at their foot (Fig. 3).

The aeolianite succession descends below sea level and the basal contact is not exposed (Fig. 4). Numerous rounded pebbles and peat are washed ashore along this coast and a cemented deposit of pebbles and marine molluscs was found in the intertidal zone at one locality, which may represent an MIS 5 beach deposit. These observations suggest that sea level was just below its present elevation when aeolian deposition commenced.

3.2. Lithology

Samples for lithological and geochronological analyses were taken at intervals from two vertical sections measured in the Pleistocene and Holocene successions in the sea-cliff exposures at Still Bay (A and B in Fig. 4). The aeolianites comprise medium-grained, moderately sorted, and variably cemented (secondary carbonate) calcarenites. They are reddish in colour (10YR7/6) with grains predominantly consisting of quartz along with comminuted shelly material (Table 2).

3.3. Dune morphology and sedimentation

Essentially, the dune cordons of the southern coast comprise vertically and laterally coalesced parabolic dunes (Martin, 1959, 1962; Tinley, 1985; Illenberger, 1996; Bateman et al., 2004). Pleistocene parabolics form prominent geomorphic features in the study area,

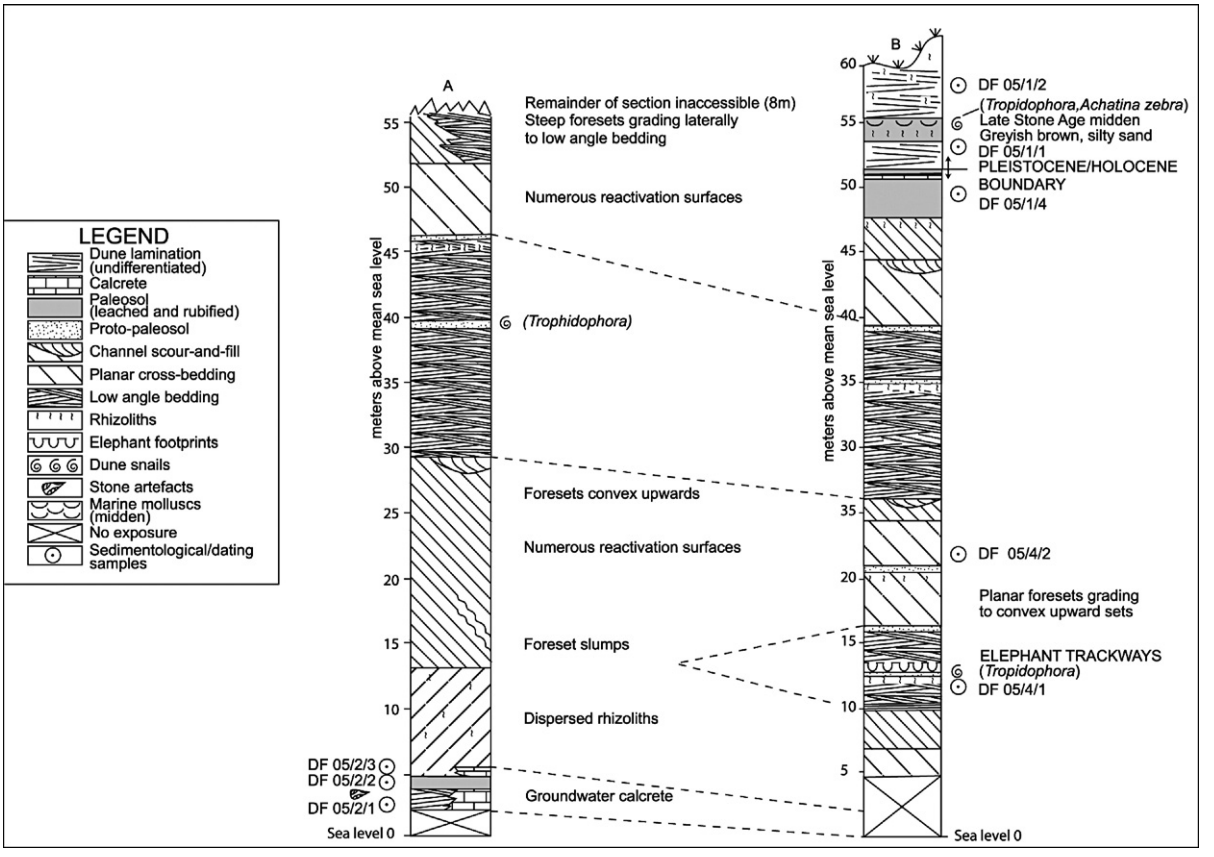

Fig. 4. Measured sections at Still Bay. For locality, see Fig. 2.

Table 2
Lithological data. See Fig. 4 for sample horizons

Field code	Munsell C. wet	% Sand	% Silt	% Clay	% Coarse	% Med S	% Fine S	Mean	Median	Sort	Skew	Kurtosis	% Carbonate	pH
DF 05/1/1	7.5YR5/4	99	0	1	5.73	73.85	20.42	1.63	1.6	0.44	0.12	0.97	6.18	9.7
DF 05/1/4	7.5YR6/6	100	0	0	10.57	58.52	30.91	1.72	1.79	0.52	−0.21	1.04	4.2	8.7
DF 05/4/1	7.5YR7/6	99	0	1	5.2	61.04	33.76	1.81	1.84	0.44	−0.13	1.12	7.26	8.8
DF 05/2/1	7.5YR6/6	97	0	3	7.59	47.93	44.48	1.81	1.91	0.55	−0.16	0.9	5.12	8.6
DF 05/2/2	5YR5/4	93	3	4	8.98	39.28	51.74	1.91	2.03	0.52	−0.25	0.84	4.71	8.9
DF 05/2/3	7.5YR6/6	98	2	0	8.06	70.01	21.93	1.61	1.65	0.46	−0.02	0.98	8.35	8.8

as seen in aerial photographs (Fig. 2) and on the ground. The most active area of present dune sedimentation occurs just east of the Goukou River with parabolic dunes forming prominent features. The Pleistocene aeolianite succession east of Still Bay, mainly comprising two major architectural elements (superposed sets of large-scale, steeply dipping planar cross bedding and low-angle lamination) is therefore interpreted in this context. From the perspectives of insight into the terrain traversed by elephants and the taphonomic processes which controlled footprint preservation, it is instructive to consider the context and sedimentation processes that gave rise to these facies.

3.3.1. Low-angle lamination

This facies comprises intersecting sets of low angle to horizontal lamination with numerous internal discordances among packages of laminae; strongly tangential bottomsets are commonplace. Bedding, which may be concave-up in places shows variable dip orientation and the contact between sets ranges from sharp and erosive to concordant. Sets range up to 2 m in thickness and may be vertically stacked; forming successions up to 4.5 m thick. Asymmetrical wind ripples are well preserved on many surfaces, with wavelengths up to 25 cm and crest heights of 1.0–1.5 cm (Fig. 5a,b). 'Pinstripe' lamination (Hunter, 1977, 1981) is a prominent

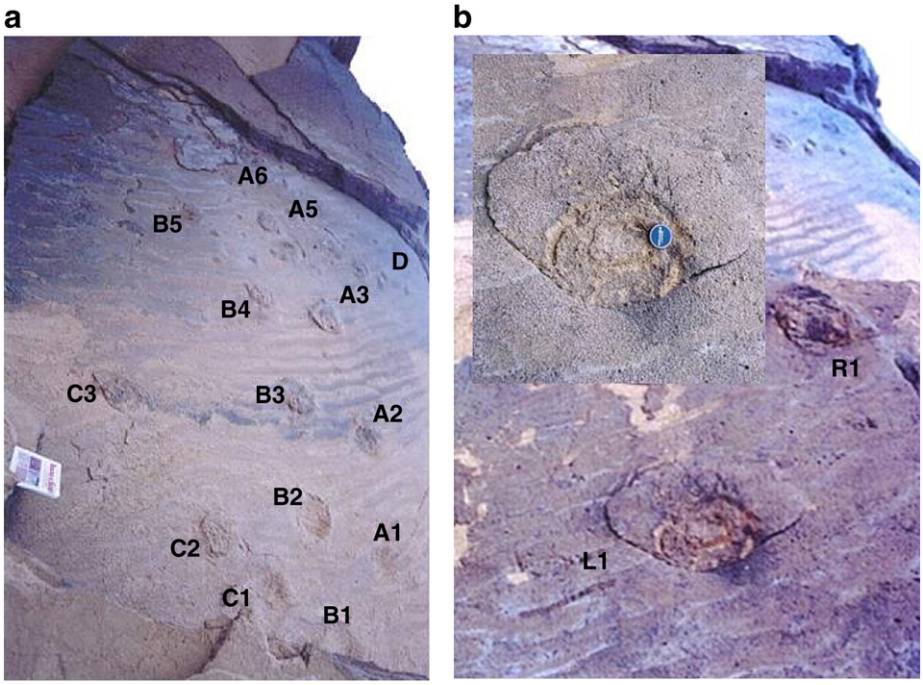

Fig. 5. (a) Three elephant trackways (A–C) traversing a palaeosurface. Two trackways (A and B) run parallel to each other, curving slightly to the left and C diverges from A and B (bottom). They are intersected by antelope trackways (D, top right). Book is 21 cm long. (b) Two well preserved elephant footprints on the upper wind-rippled surface of the same aeolianite slab as in (a). The round L1 impression (pes) is situated within a perfectly preserved wedge of substrate displaced by the footfall. R1 is blurred due to a sliding motion of the foot. Inset shows a close-up of the L1 footprint.

feature (Fig. 6a). This facies may be laterally persistent and the example shown in Fig. 3 was traced in an east–west direction for over 300 m before disappearing behind rockfalls. Elephant and other vertebrate trackways are most abundant in this facies (Fig. 6a–c).

The typical lateral persistence and appreciable thickness of the low-angle laminated facies reflects deposition on broad, stable, generally subdued topographies, probably interdune areas (Hunter, 1977; Fryberger et al., 1979; Hunter, 1981). These coast parallel features are extensively developed between dune cordons in modern and ancient south coast dunefields. The low-angle facies is largely a product of wind ripple migration and grainfall; foreset dips are too low to induce grain flow (Hunter, 1977, 1981). This interpretation is underpinned by the well preserved ripples and 'pinstripe' laminae (Fig. 6a), resulting from ripple migration (Hunter, 1977; Fryberger et al., 1979; Hunter, 1981). A similar facies in carbonate aeolianite on San Salvador, Bahamas was described and largely attributed to amalgamated wind ripple migration deposition (Caputo, 1995).

3.3.2. Large-scale foresets

Planar cross-bedded units ranging in thickness from 0.4–24 m are the dominant primary sedimentary structure in the succession. The large-scale units (>2 m) may be laterally persistent for tens of meters with foresets dips of up to 37°. The foresets are mostly tabular, but may also be concave-up or convex up and some are complex with internal cross-bedding; bottomsets are tangential to angular in form (Fig. 3). Reactivation surfaces, marked by erosional disconformities or changes in foreset orientation and/or dip angle, are ubiquitous. The foresets typically comprise alternating thicker (up to 25 cm), coarser-grained, lighter-coloured, sharp-based laminae bounded by bundles of thinner, darker coloured laminae

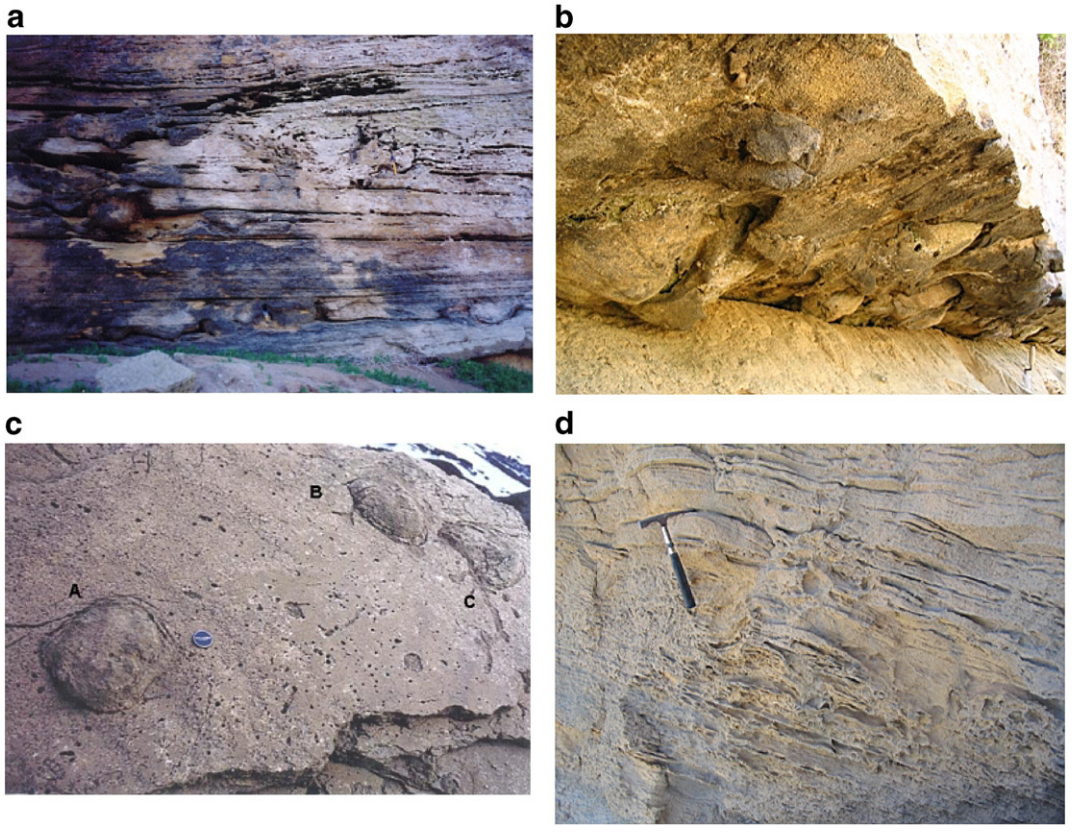

Fig. 6. (a) Superposed trampled horizons at site C (downward bulges are elephant footprints). Cliff is 3.5 m high. (b) Elephant footprints at site C exposed as casts on the underside of the main elephant trackway horizon, overlying a soft protosol (see Fig. 4). The bed is so heavily trampled that the prints overlap (trowel handle is 9 cm long). (c) Fallen sandstone block bearing three elephant footprints as casts. Footprint A has the broadly oval outline typical of the hindfoot of *L. africana*. Footprints B is round, typical of the manus (forefoot); the footprint on the right incomplete. Lens cap 5 cm across. (d) Deep disturbance of substrate by an Elephant footprint seen in vertical section (immediately right of 30 cm long Hammer) on steeply dipping foresets (~32°; note that the dip of ~20° as seen in the figure is the apparent dip). Thicker foresets are separated by thinner, negatively weathered laminae.

which weather negatively (Figs. 3 and 6d). Some thicker foresets are broadly lenticular in form both along strike and down dip, clearly wedging out into pinstripe laminae. Vague internal lamination is also apparent in some of the thicker foresets (Fig. 6d). The thinner laminae show more continuity and in places are internally cross-laminated with wind ripples preserved in places.

Large-scale, steeply dipping planar cross-bedded units (Fig. 3) represent progradation of major dune slipfaces in the nose and trailing arms of parabolic dunes, mainly under the influence of prevailing winds (Hunter, 1977; Sweet, 1992; Illenberger, 1996). Convex up foresets (Fig. 3) are commonly associated with recent and Quaternary parabolic dunes and are formed in the nose region of hairpin parabolic dunes (McKee, 1966; Adams, 1983; Caputo, 1995). Smaller-scale planar cross-bedding represents migration of smaller bedforms, commonly superimposed on the larger features (Hunter, 1977; Illenberger, 1996).

The thicker bedded foresets (Figs. 3 and 6d) with vague internal lamination showing lateral continuity along depositional strike are suggestive of grainfall sedimentation (Hunter, 1977, 1981; Sweet, 1992; Caputo, 1995). Packages of thinner 'pinstripe' laminae are regarded as amalgamated wind ripple sets (cosets), produced by prevailing winds and eddies which may be oriented at large angles to the prevailing direction (Hunter, 1977; Sweet, 1992; Caputo, 1995). The large-scale, steeply dipping planar cross-bedded facies therefore displays all three of the main aeolian sedimentation processes (grainfall, ripple migration and grainflow) proposed by Hunter (1977). Trace fossils (Fig. 6d) are rare in this facies.

The palaeowind analysis included only large-scale (>2 m), steeply dipping cross-stratification (>30°) with a significant grain flow component. Smaller and shallower dipping structures may represent sedimentation by ripple migration and grainfall by wind eddies on surfaces oriented at large angles to prevailing palaeowinds (Sweet, 1992). The 83 measurements summarized in Fig. 7 illustrate the dominance of winter westerly winds (Kruger, 2004) in dune formation. This is confirmed by the orientation of currently active and fossil parabolic dunes in the study area (Fig. 2), as well as Late Pleistocene lunette dune orientation on the Agulhas Plain (Carr et al., 2006a,b). It appears that Late Pleistocene palaeowind patterns and their influence on dune morphology are similar to those of the present.

3.4. Palaeosols

Ancient soils, commonly called 'palaeosols' (Kraus, 1999; Retallack, 2001) mark breaks in dune sedimentation and as such are germane in piecing together the depositional history and controls on dune deposition. Samples bracketing the major palaeosols (P1 and P2) were therefore taken in order to assess their temporal significance (Fig. 4). Palaeosols are dispersed throughout the aeolian succession at Still Bay and the degree of pedogenesis ranges from slight to intense. They undulate to varying degrees in three dimensions, reflecting former abandoned dunefield topographies (Barwis and Tankard, 1983). Soil profiles on dunes develop only after their colonisation and stabilization by vegetation (Knox, 1977; Bowman 1979; Thompson, 1981; Roberts and Brink, 2002).

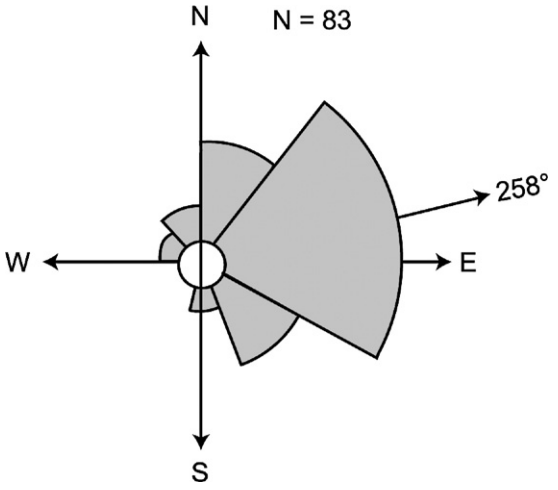

Fig. 7. Rose diagram showing the 83 measurements of large-scale, steeply dipping foresets. The pattern illustrates the dominance of westerly winds in dune formation, with only minor components from the east.

Incipient paleosols (protosols) are the most common form at Still Bay. Primary bedding is homogenized over a narrow interval (20–50 cm) and although rhizoliths (Klappa, 1980) and fossil dune snails may be present, little detrital carbonate leaching or sediment discolouration is evident (Fig. 3). This type of palaeosol tends to be laterally discontinuous and probably represents a relatively brief and localised pause in sedimentation (Knox, 1977). More mature profiles are marked by leaching of detrital carbonate, bleaching, rubification, ferricretisation, calcretisation and intense concentration of rhizoliths, over intervals of up to 5 m. Only two well developed, laterally persistent palaeosols (P1 and P2) were encountered in the ~60 m thick aeolianite succession at Still Bay (Fig. 4). The terminology of Birkland (1984) is used in the following descriptions.

The oldest example (P1) occurs near the base of the succession and ranges from 1.2–2.2 m in thickness. It

could be traced intermittently over ~6 km, but dips below present sea level in the east. In the vicinity where vertical section 'B' was measured (Figs. 2 and 4), a leached and bleached 15–30 cm thick 'E' horizon grades downwards into a rubified 'Bo' horizon (30–80 cm), which in places is transitional into an underlying lighter-coloured horizon. This rests with an irregular contact on root bioturbated, partly weathered calarenite ('C' horizon) which grades down into laminated, unweathered aeolianite with rhizoliths (Fig. 8a). No organic 'O' or 'A' horizon is present. In some areas, P1 is only represented by a rubified 'Bo' horizon with laterally persistent, sub-horizontal, wavy, heavily iron-stained ('liesegang') laminae, suggesting a high water table. The small dune snail *Tropidophora* sp. occurs in abundance, as intact specimens and as comminuted accumulations. Aeolianite calcification is more intense above and below P1. The absence of pedogenic features and down slope-orientated fabric suggests groundwater flow as the agency that produced this feature.

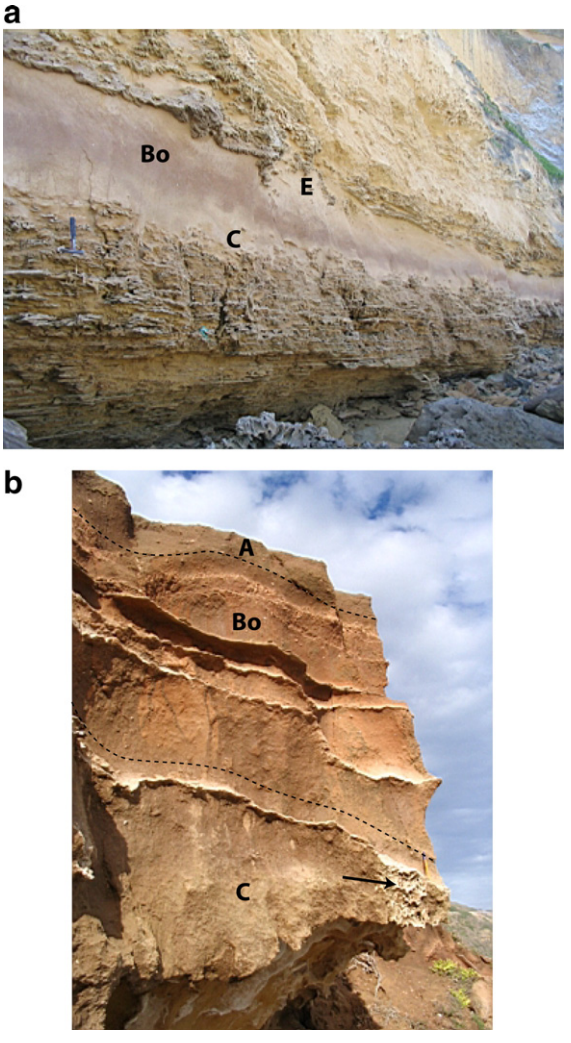

Fig. 8. Palaeosols exposed at Still Bay. (a) The P1 palaeosol showing a leached and bleached A2 horizon grading downwards into a rubified B horizon (30–80 cm), transitional into an underlying bleached horizon; note intense calcification above P1 and rhizoliths below. (b) The P2 palaeosol with A1 horizon of dark brown sand, underlain by a well developed, rubified B horizon. Note the thin, undulating, laminar calcretes (3–20 cm thick) and termite nest below and left of 15 cm long pen (bottom right).

A second mature palaeosol (P2) caps the aeolianite succession at Still Bay. It displays a pronounced undulating character and can be traced along the entire belt of outcrop. P2 ranges up to 5.5 m in thickness within swales, but may thin to as little as 1.2 m over topographically positive areas. The thicker palaeosols typically comprise a thin 'A' horizon of dark brown, slightly organic, quartzose sand, underlain by a well developed, decalcified and rubified 'Bo' horizon up to 1.5 m thick (Fig. 8b). Thin, wavy calcrete laminae are typically developed within the 'Bo' horizon. The latter grades downwards into less weathered, yellowish brown sands with numerous calcareous rhizoliths ('C' horizon), which are in turn underlain by unweathered aeolianite exhibiting primary sedimentary structures. The small dune snail *Tropidophora* sp. and larger *Achatina zebra* is common in P2 and fossil termite nests were also observed (Fig. 8b). P2 may in places be dominated by a laminated calcrete or 'K' horizon, especially where it thins over topographic highs.

At locality 'A' (Fig. 2) a ~3 m thick cross-bedded unit is extensively iron-stained with laterally persistent, sub-horizontal, wavy to convoluted 'liesegang'-type bands and laminae near the base of the succession (Fig. 9). The foresets are poorly defined ('fuzzy') and more wavy in form than typical aeolian cross-beds. The characteristic dune snails *Tropidophora* sp. and *Achatina zebra* are replaced by a small (0.8 cm) mollusc shell with a distinctive recurved apex, identified as the internal skeleton of the extant brackish-water slug *Ferissia* sp. The sub-horizontal 'liesegang'-type banding is suggestive of generally high, but variable water tables. The pale colouration and replacement of terrestrial dune snails by the brackish-water slug suggests wet, reducing conditions. This site is adjacent to the present interdune wetland Rietvlei (Fig. 2) and it appears that a similar water source was active in this area during the Late Pleistocene.

4. Dating

4.1. Optically stimulated luminescence (OSL)

All OSL samples were obtained by hammering opaque plastic tubes into exposed sections. Coarse grained quartz

Fig. 9. Poorly defined ('fuzzy') 3 m thick foresets (base of sequence) with 'sub-horizontal to convoluted 'liesegang'-type banding. The presence of the extant brackish-water slug *Ferissia* (not shown) suggests wetland conditions.

(150–250 μm) was extracted following the methodology of Bateman and Catt (1996). Measurements were carried out on a Risø TL/OSL DA-15 automated luminescence reader (samples Shfd05010-Shfd05014 inclusive; stimulation with blue diodes for 50 s at 125 °C) or a Risø TL/OSL DA-12 reader using a Halogen lamp (filtered with a 150 W lamp filter and a green long-pass Schott GG-420 filter) for 80 s at 125 °C (samples Shfd05006 and Shfd05009). The resulting luminescence signal from both stimulation sources was measured via a Hoya U-340 filter + SWP interference filter. Irradiation was supplied by a ^{90}Sr-^{90}Y β source.

Equivalent doses (D_e) were determined using the single aliquot regenerative dose protocol (SAR; Murray and Wintle, 2000) using five regenerative doses (including a repeat point "recycling ratio" dose). Preheat plateau tests were conducted on samples Shfd05012 (Pleistocene) and Shfd05006 (Holocene). The latter sample displayed limited sensitivity to preheat temperature in the range 160–260 °C and recuperation was less than 0.5% of the natural signal for all temperatures below 240 °C. No significant trend in D_e with preheat was observed for Shfd05012 over the same temperature range. Checks for IR contamination were made following the depletion ratio method of Duller (2003). Dose recovery experiments were conducted on six samples (Murray and Wintle, 2003). The average ratio of administered: recovered dose was 1.02 ± 0.05 (n = 17), suggesting that good precision and accuracy have been obtained, with minimal sensitivity change prior to the administration of the first test dose. All of these aliquots recovered a dose within 5% of the administered dose. Growth curve fitting (exponential plus linear) was conducted using the "Analyst" software and averaged D_e determinations were derived with the "central age model" of Galbraith et al. (1999).

Dose rates were determined via in situ gamma spectroscopy (GS) with the exception of sample Shfd05007 for which inductively coupled plasma mass spectrometry (ICP-MS; performed at SGS laboratories, Canada) was utilized. Elemental concentrations were converted to dose rates using the data provided by Aitken (1985) and Marsh et al. (2002). Cosmic dose rate contributions were calculated following Prescott and Hutton (1994). The use of present-day sample depths in calculating the cosmic dose was deemed inappropriate, since initial calculations of OSL age estimates showed that episodic sedimentation had taken place over an extended time period. This problem was addressed by the application of an age-depth model to account for changing burial depth with time. Approximate ages for the different samples were determined incorporating a cosmic component calculated as per Prescott and Hutton (1994). Using a top-down approach, these ages were then used to establish a burial depth history for each sample. Using this sample burial depth history (rather than present day depth), cosmic doses were recalculated and applied to the final age calculations. Whilst this approach takes no consideration of possible erosional events, it models actual burial history more accurately than the usual approach whereby it is assumed that entire sedimentary

sequences were deposited synchronously. Results are shown in Table 3.

Samples bracketing and including the lower palaeosol (P1) (Shfd05010 to Shfd05012) underwent more detailed dosimetric analysis using GS, thick source alpha counting (TSAC) and ICP-MS as the potential for radioactive disequilibrium/heterogeneity was thought to be much higher. These comparisons show excellent agreement between methods for sample Shfd05012, but considerable variability for sample Shfd05010. GS (measuring daughter isotopes) is consistently lower than TSAC/ICP-MS for Th but similar for U. This could mean that unlike U the ^{232}Th chain is in disequilibrium, although this is very unusual in natural sedimentary deposits (Olley et al., 1996). Both TSAC and GS results show U:Th ratios mostly less than 1:2, indicative of some U enrichment, which reflects the marine origin of the carbonate content of the sediment. Some differences are apparent in the K concentrations between GS and ICP. This cannot be due to disequilibrium (as GS directly measures ^{40} K). Poor K uptake during ICP fusion seems unlikely and data derived by this technique usually show excellent consistency (e.g. Carr et al., 2007). This evidence suggests that the differences between methods are more likely to reflect sediment heterogeneity and related sub-sampling issues, within and below the palaeosol. This may be particularly significant for sample Shfd05010, which could only be obtained from a unit containing sporadic carbonate nodules, many of which were within a ~0.5 m radius of the sampling hole.

For age calculation all dose rates for samples Shfd05012-Shfd05010 are based on GS data. For the problematic sample Shfd05010, this technique will incorporate the effects of spatial variation in the dose rate and will also measure the modern dose rate, regardless of the state or degree of disequilibrium. It is unclear at what stage any carbonate nodule formation would have occurred, although if this happened soon after deposition (e.g. when meteoric waters were available for such processes) the GS dose rate may be a reasonable reflection of the average burial dose rate.

4.1.1. Results

Details of the OSL analyses of the seven samples are presented in Table 3. The OSL dating reveals a range of ages from ~143 ka to 8 ka. The three samples bracketing and including the well developed palaeosol P1 (see Section 3.3; Figs. 4 and 8a) produced ages of 114±6.8, 121±6.5 and 126±7.1 ka (Shfd05012, Shfd05011 and Shfd05012). These ages are compatible with the stratigraphy and suggest that the lower part of the succession relates to Marine Isotope Stage (MIS) 5e. The samples from section B (Fig. 4) are also concordant with the stratigraphy, as the samples bracketing the main elephant trackway horizon gave ages of 140±8.3 ka and 136±8.4. The sample from below palaeosol P2 dates to 91±4.6 ka (shfd05009) and provides a maximum age for this well developed palaeosol. The early Holocene age of 8.6±0.4 (Shfd05006) from the unconsolidated dunes of the Strandveld Formation indicates a considerable hiatus in deposition across P2 (Figs. 4 and 8a).

Table 3
Details of the Still Bay OSL age determinations (∗ U, Th and K determinations by ICP-MS; † cosmic dose negligible due to thickness of overburden

Sample details			Dosimetry						Palaeodose		OSL age
Lab code (field code)	Horizon	Depth (m)	Alpha (μGy a^{-1})	Beta (μGy a^{-1})	Gamma (μGy a^{-1})	Cosmic dose (μGy a^{-1})	Water content (%)	Total dose rate (μGy a^{-1})	Aliquots	D_e (Gy)	(ka)
Shfd05006 (DF05/1/1)	Above upper calcrete P2	3	10±2	243±22	249±17	194±10	1.1	697±29	16	5.98±0.10	8.6±0.4
Shfd05009 (DF05/1/4)	Below upper calcrete P2	4.3	7±1	207±19	194±13	173±9	4.8	581±24	15	53.1±1.5	91±4.6
Shfd0514 (DF05/4/2)	Above elephant tracks	38	7±1	195±18	190±12	18±1	6.8	410±22	8	58.6±1.5	136±8
Shfd0513 (DF05/4/1)	Below elephant tracks	48	5±1	157±16	148±10	–†	3.8	311±18	17	44.5±1.1	140±8
Shfd05012 (DF05/2/3)	Above palaesol P1	78.5	7±1	201±18	193±13	–†	4.4	401±22	14	45.0±1.0	114±7
Shfd05011 (DF05/2/2)	Palaeosol P1	81	15±3	323±26	341±22	–†	7.9	679±34	13	82.4±1.5	121±7
Shfd05010 (DF05/2/1)	Below palaeosol P1	82	8±2	244±21	234±15	–†	5.3	487±26	14	61.8±1.1	126±7

See Fig. 4 for sample horizons.

4.2. Amino acid racemization (AAR)

4.2.1. Methods

The degree of racemization of amino acids, a measure of fossil age based on the increasing ratio of D to L-amino acids, was determined in fossil molluscs and "whole-rock" sediment samples by Reverse Phase, High Performance Liquid Chromatography following the methods of Kaufman and Manley (1998). Analyses were undertaken on the total hydrolysable amino acids, after hydrolysis for 22 h at 110 °C in 8 mol HCl. The analytical procedure involved the pre-column derivatization of DL-amino acids with *o*-phthaldialdehyde (OPA) together with the chiral thiol, *N*-isobutyryl-L-cysteine (IBLC) to yield fluorescent diastereomeric derivatives of the chiral primary amino acids. Amino acid D/L ratio determinations were undertaken using an Agilent 1100 HPLC with a C-18 column and auto-injector. Results are reported for the amino acids glutamic acid and valine.

From the Late Pleistocene aeolianite succession (Waenhuiskrans Formation), the terrestrial gastropod *Tropidophora* sp. was analysed from the basal palaeosol (P1, Fig. 8a) and immediately below the main elephant trackways (Figs. 3 and 4). Three AAR whole-rock sediment samples were collected (250 μm to 500 μm sedimentary particle fraction) from below the basal P1 palaeosol, directly below the main elephant trackways and ~10 m above this horizon (Fig. 4; Table 4).

4.2.2. Results

The highest degree of racemization is observed in the basal aeolianite beneath the P1 palaeosol and shows that the carbonate grains within this unit were formed significantly earlier than the superposed units with the trace fossils (Figs. 4 and 8a; Table 4). Specimens of terrestrial gastropods from the basal palaeosol (P1) and aeolianite immediately below main the elephant trackway yielded lower degrees of racemization relative to the Pleistocene aeolianite. The degree of racemization within these fossils is a more representative indicator of the overall rate of racemization with time over the course of the Late Pleistocene, as the higher degree of racemization determined in the aeolianites reflects the presence of relict skeletal carbonate grains derived by sediment re-working before their final deposition.

The D/L values for valine from the Late Pleistocene aeolianites are of a similar order of magnitude to those determined for the amino acid leucine (which undergoes a similar rate of racemization to valine) for Last Interglacial aeolianite from the Coorong Coastal Plain in southern Australia (Murray-Wallace et al., 2001). In the latter region, the relict skeletal carbonate grains are derived from erosion of aeolianites deposited in the previous interglacial maximum [i.e. Oxygen Isotope Stage 7 (OIS) skeletal carbonate sediment being incorporated in sediments during the Last Interglacial (OIS5e)]. In a similar manner, it appears that the Last Interglacial aeolianite succession at Still Bay contains a significant proportion of reworked material derived from a Middle Pleistocene source, accounting for the higher degree of racemization in these sediments.

4.3. Synthesis

The whole-rock AAR below P1, the basal palaeosol (UWGA-5398A-C, Table 4) suggests a greater age than for the two whole-rock AAR samples above and below the main elephant trackway (UWGA-5399A-B and UWGA-5400A-C, Fig. 4; Table 4). The same conclusion can be drawn for glutamic acid in the terrestrial gastropods associated with these horizons (valine is about the same). The main elephant trackway stratigraphically overlies the P1 palaeosol (Fig. 4), and should be younger, so the AAR is concordant with the stratigraphy. The whole-rock AAR

Table 4
Extent of amino acid racemization (total hydrolysable amino acids) in "whole-rock" sediment samples and fossil molluscs. See Fig. 4 for sample horizons

Horizon/sample code	Lab code	Material	OSL age (ka)	D/L valine	D/L glutamic acid	Number of replicate
Aeolianite above elephant tracks (DF05/4/2)	UWGA-5400A-C	Whole-rock	136±8.4	0.528±0.020	0.485±0.004	$n=3$
Immediately below elephant tracks (AAR # 5: DF05/4/1 horizon)	UWGA-5225A-C	Dune snail (*Trophidophora* sp.)	140±8.3	0.386	0.48	$n=1$
Aeolianite below elephant tracks (DF05/4/1)	UWGA-5399A-B	Whole-rock	140±8.3	0.546±0.013	0.475±0.001	$n=2$
P1 basal palaeosol (AAR # 4: DF05/2/2 horizon)	UWGA-5225A-C	Dune snail (*Trophidophora* sp.)	121±6.5	0.379±0.103	0.576±0.075	$n=3$
Basal section below P1 palaeosol (DF05/2/1)	UWGA-5398A-C	Whole-rock	126±7.1	0.623±0.011	0.493±0.016	$n=3$

above and below the main trackway are similar, as expected given the absence of evidence for stratigraphic breaks between the samples. The OSL samples bracketing and including palaeosol P1 (Shfd05010 to Shfd05012) are compatible with MIS 5e (Fig. 4; Table 3). As noted above, sea level was apparently only just below the present level at the onset of aeolian deposition, underpinning these ages. The sample above the basal palaeosol relates to the MIS 5e–5d transition. The OSL ages of the samples bracketing the main elephant trackway horizon are greater than those relating to the stratigraphically older P1 palaeosol, representing a minor age inversion. They could nonetheless be interpreted as of a very early MIS 5e age (Fig. 4; Table 3). The OSL dating, with consideration of errors (quoted in Table 3 as 1 sigma) is thus also broadly concordant with the stratigraphy and is indicative of MIS 5 deposition.

Dating of Holocene palaeosols in Western Australia indicate that the degree of pedogenesis observed in profiles P1 may develop over a few thousand years (Thompson, 1981). The OSL dates bracketing the P1 profile indicate a maximum age of ~10 ka for its genesis (Figs. 4 and 8a). The depositional age of ~122 ka from the P1 profile itself suggests a period of ~7 ka, since pedogenesis would have been ongoing until terminated by the subsequent phase of sedimentation dated to ~115 ka. Profile P2 is generally much thicker and more mature than P1 (Fig. 8a and b). The OSL age of the unweathered aeolianite below palaeosol P2 is ~91 ka, whereas the overlying aeolian sediments date to the Holocene at ~8 ka. These age relationships show that pedogenesis may have persisted until terminated by deposition of the overlying Holocene dunes i.e. for ~80 ka, consonant with the relative maturity of the P2 profile and its lateral persistence (assuming that there was no earlier aeolian deposition and erosion prior to ~8 ka). This prolonged period of sediment starvation is coincident with glacioeustatic-driven shoreline retreat; preservation of Late Pleistocene aeolianites offshore on the Agulhas Bank record dune sedimentation. Bateman et al. (2004) have recorded dune deposition between 60–90 ka elsewhere along the southern coast, but aeolian deposition at the present time is concentrated along the modern strandline.

5. Elephant trackways

5.1. Description and interpretation

Elephant footprints occur in abundance in the calcified Late Pleistocene aeolianites east of Still Bay. Five occurrences, varying from a few footprints to intensely trampled surfaces along a ~3 km coastal stretch of aeolianite exposures are described here (Fig. 2). The footprints occur in situ as well as in loose blocks fallen from the coastal cliff. They may be seen in profile, as casts on the underside of beds and as natural impressions on palaeosurfaces.

5.1.1. Site 1

At site 1 (Fig. 2), elephant trackways are superposed over a vertical interval of ~4 m in a steep cliff face (Figs. 3 and 6a). Successive sediment increments were trampled, recording a game trail that was utilized repeatedly over an extended time period. At the base of this footprint-bearing succession, a recess has been formed by wind scour in a soft decalcified bed (protosol), exposing many footprints as casts on the underside of the overlying, well cemented bed (Fig. 6b). This exposure extends over a horizontal distance of ~33 m. The bed is so heavily trampled that the prints overlap and individual trackways are lost among the numerous, sometimes merged footprints, suggesting that a sizable herd of elephants traversed this palaeosurface. No accurate measurement of footprint dimensions was feasible at site 1.

5.1.2. Site 2

At site 2 (Fig. 2), a fallen sandstone block 2.7×1.7×0.8 m in the intertidal zone bears three elephant footprints, well preserved as casts on what was the underside of the bed (Fig. 6c). The push-up mounds are symmetrical around the impressions, suggesting that the original slope of the surface was slight. Footprint A (Fig. 6c) has the broadly oval outline typical of the pes (hindfoot) of *Loxodonta africana* with a slight anterior bulge (Stuart and Stuart, 1994) indicating the animal's direction of progression from left to right. The maximum relief (depth of the original impression) is 11 cm; the longer dimension is 38 cm and the shorter one 27 cm.

Footprint B is almost round in form (33 cm diameter); typical of the manus (forefoot) and the maximum relief is 9 cm. Because footprint C is only partially preserved, its dimensions cannot be accurately measured; a more distinct push-up mound surrounds this print. It possible that A and B represent the pes and manus of a single trackway (the distance between them is 120 cm), but the trackway is too short to be certain of this. Footprint C is offset relative to A and B and is unlikely to have been made by the same animal. The long axis of the broadly oval pes (hindfoot) can be used to estimate elephant shoulder height and age (Figs. 10 and 11; Western et al., 1983). The dimensions of footprint A indicate an animal with shoulder height of

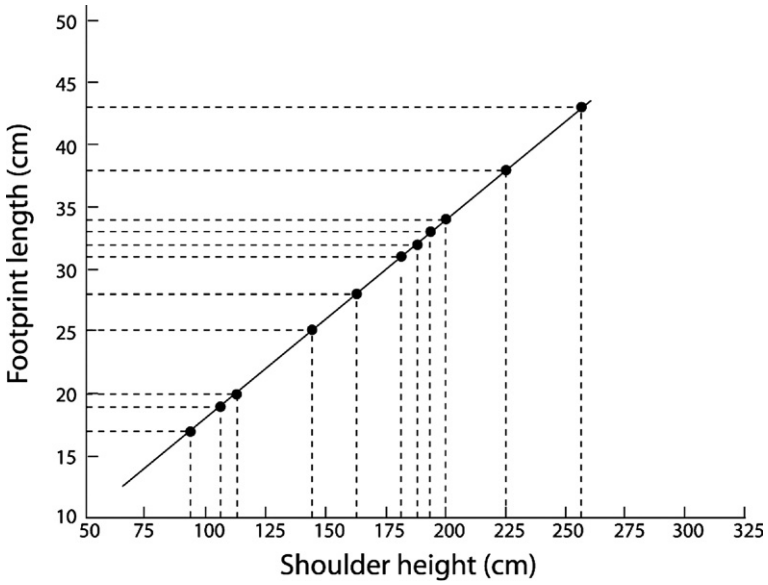

Fig. 10. East African data relating the dimensions of the long axis of the oval pes (hindfoot) of *L. africana* to shoulder height (Western et al., 1983). The filled circles represent the Still Bay elephants.

~225 cm and an age of ~13–14 years; i.e. a large but not yet fully grown animal.

5.1.3. Site 3A

A series of well preserved footprints feature as natural impressions on exposed, wind-rippled surfaces of a large (5.0 × 3.5 × 0.3 m), fallen aeolianite slab which is almost vertically oriented. The dimensions of the upper bed are 1.8 × 1.6 m × 0.09 m (the remainder had been broken off) on which two elephant footprints are well preserved as natural impressions. Asymmetrical wind ripple preservation on this surface is poor relative to the underlying bed, but the wavelength (~20–25 cm) and crest heights (1.5–2.2 cm) could still be measured (Fig. 5b). The footprints are 1.2 m apart and appear to form part of the same trackway. L1 comprises a 25 cm-

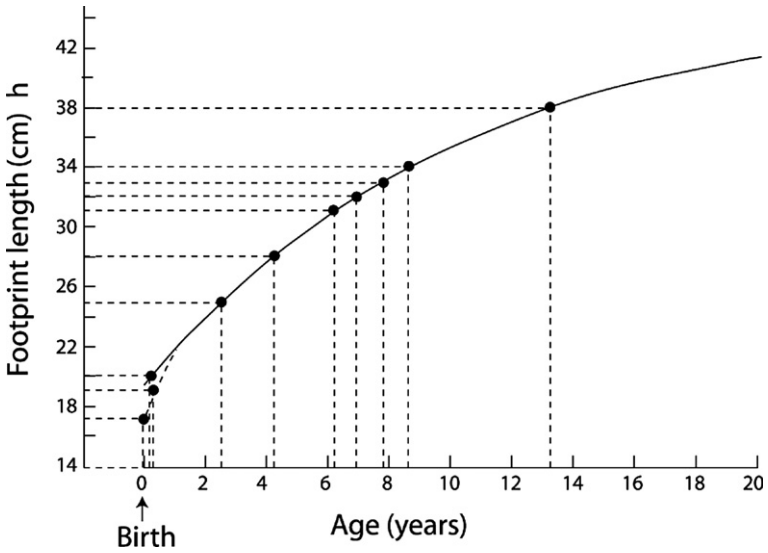

Fig. 11. East African data relating the dimensions of the long axis of the oval pes (hindfoot) of *L. africana* to age (Western et al., 1983). The filled circles represent the Still Bay elephants.

wide, approximately circular foot impression (Fig. 5a,b) with no visible toe marks. A 3 cm high 'cliff' (referred to as the 'wall' by Brown, 1999) surrounds the impression, resulting from displacement/compaction of sediment within the foot impression.

The L1 and R1 footprints are about 75 cm apart. The L1 impression is situated within a large (63×40 cm), perfectly preserved wedge of substrate displaced by the footfall. This sediment wedge truncates the wind ripples, showing that the ripples formed prior to the passage of the elephants. The surface behind the foot impression is slightly depressed. L1 is 25 cm in diameter and its rounded form indicates that it is the pes. R1 is blurred and appears elongated, with displaced wedges of sand *within* the impression (Fig. 5b) indicating a downslope sliding motion of the foot (Brown, 1999) and is probably the manus.

Adding 15% to the 25 cm diameter of L1 (see above) yields an approximate pes length of ~28 cm (R1 is too blurred to measure). This indicates an animal with shoulder height of ~160 cm and an age of between four and five years (Figs. 10 and 11). The poor wind ripple preservation contrasts with the excellent detail of the elephant footprints and with the well preserved wind ripples on the underlying bed (Fig. 5a,b). As noted above, the ripples formed prior to the passage of the elephants. The cohesive character of the displaced wedge of sand associated with L1 suggests that the substrate had been well moistened by rain before the footprints were made, which could also explain the degradation of the ripples.

5.1.4. Site 3B

In Fig. 5a, the part of the rock slab bearing the well preserved prints shown in Fig. 5b has detached, revealing the continuation of the underlying trackways. The darker hue of the left-hand part of the surface is due to denser algal/lichen growth than the more recently exposed, naturally coloured aeolianite on the right. Because of the near vertical orientation of the rock slab, only the lower footprints in Fig. 5a were available for direct study. The surface is criss-crossed by elephant and other mammalian trackways. It is also mantled by well preserved, bifurcating, asymmetrical wind ripples with wavelengths of ~20–25 cm and crest heights of 1.0–1.5 cm. The ripple crests are parallel to those of the overlying bed and the steeper lee face is on the same side (towards the bottom of the photo). The ripples also are overprinted by the trackways and so formed prior to them.

Three elephant trackways (A, B and C) traverse this surface. Two trackways (A and B) are oriented almost normal to the strike of the ripple crests and run parallel to each other, curving slightly to the left (Fig. 5a). They are intersected and overprinted by at least two sets of antelope trackways (D) at the top right of Fig. 5a and are therefore younger than either. Trackway C diverges from A and B in the bottom right of Fig. 5a at an angle of ~30°. The shallow impressions suggest that the sand was well compacted and had been deposited at an appreciable time interval before the impressions were made. The narrow stride width characteristic of proboscidians with the limbs tending to swing below the body is evident in all three trackways (Leaky and Harris, 1987; Hutchinson et al., 2003).

Elephant footfall pattern is LP-LM-RP-RM (M=manus; P=pes; L=left; R=right) i.e. the fore and hind foot on the same side are swung forward simultaneously (Hutchinson et al., 2003). There is also a tendency for overprinting of the pes by the manus (Leaky and Harris, 1987). Trackway 'A' comprises 6 prints with an average stride length of 65 cm. A4 is an exception, and is only 25 cm from A5. Clear asymmetric push-up mounds are developed in A2 and A3. A3 appears oval in form and is taken to be the pes with a diameter of 17 cm. Trackway B comprises 5 prints also with an average stride length of 65 cm. B2 is better preserved than the other prints, appears oval in form and is taken to be the pes, with a diameter of 20 cm. Toe marks are not generally visible in elephant footprints (Stuart and Stuart, 1994), but two can be discerned on the right of B2, demonstrating that progression was from bottom to top in Fig. 5a. Asymetrical push-up mounds are developed in B3 and B4. Trackway C 3 comprises 3 prints with a stride length of 70 cm between C2 and C3, but only ~25 cm between C1 and C2. The diameter of the oval C2 print is 19 cm and an asymmetric push-up mound is developed in C2.

The intermittent shorter stride lengths seen in trackways A and C illustrate a change in gait. The parallelism of trackways A and B, even through the curvature, suggests two (very young) animals walking side by side and influenced by mutual behaviour. Trackways C could record the meanderings of A or B but more likely an additional individual which made up a group of three elephants. The A, B and C trackway indicate very young animals with shoulder heights of ~110 cm and ages of <1 year (Figs. 10 and 11).

The asymmetrical push-up mounds seen in all three elephant trackways, as well as the two prints of Site 3A, record directed pressure (Brown, 1999). The site 3A trackway stratigraphically overlies Site 3B trackways and is approximately parallel to them (Fig. 5b). All the asymmetric push-up mounds are situated on the same side of the prints. In footprint B2, the direction of progression can be deduced from the toe marks i.e.

bottom to top of Fig. 5a. It can therefore be concluded that these features were produced by directed pressure induced by downslope locomotion (sliding motion) and also that the in situ dip of the beds was approximately normal to the strike of the ripple crests.

5.1.5. Site 4

At this site which is 35 m above mean sea level (amsl) in a cliff face, elephant footprints are seen only in vertical section on steeply dipping foresets ~(25–32°) with set thickness of ~4 m (note that the dip of ~20° as seen in Fig. 6d is the apparent dip). Footprints made on such steeply dipping surfaces show the deepest disturbance of the substrate (ranging up to 30 cm, Fig. 6d). This may be a consequence of unequal weight distribution upon the limbs due to the abnormal gait adopted to negotiate a steep and unstable substrate (dune face) and/or undercompacted sand.

5.2. Taphonomy

Only dune sand moistened by rain or dew has the cohesion to preserve anatomical detail of footprints (McKee, 1944; Roberts and Berger, 1997; Roberts, in press). The rich, frequently well preserved ichnofauna dispersed throughout the Late Pleistocene aeolianite succession at Still Bay suggests frequent moistening of the dunes by rainfall, promoting good footprint preservation (in keeping with the present climate with year-round rainfall, Fig. 1). Because of the depth and degree of sediment disturbance caused by some elephant footprint impressions, undertracks and overtracks are common on exposed surfaces in the study area. Sediments adjacent to the footprints may also display a general disturbance (Fig. 6d).

According to a model for footprint preservation in the coastal aeolian environment (Roberts, in press), prevailing winds (westerly in the Still Bay region) dry out and mobilise sand on the windward aspect of bedforms. On the protected lee face, the sand remains damp and cohesive, conferring resistance to erosion to features such as footprints. Sand blown from the windward aspect infills and buries footprints via the processes of grainflow (steep slopes) and grainfall (Hunter, 1977, 1981). Footprints on the windward side of the bedform would be subject to desiccation and erosion and therefore their preservation potential is low. Since dune sedimentation is effected mainly by (winter) westerly winds in the Still Bay region (Fig. 7), it follows that footprints were probably preserved predominantly during the winter months.

The notable thickness of foresets in the study area (up to 24 m) illustrates that the elephants traversed a landscape characterised by large dune forms, probably partially vegetated parabolic dunes; as at the present time. The elephant footprints, as well as other mammalian trackways at Still Bay are commonly associated with the low-angle bedded facies, thought to represent mainly broad, gently undulating, interdune topography. The fauna may have traversed this terrain in preference to steep, unstable dune faces. The sand laminae of the low-angle bedded facies dip at angles too low for grainflow (avalanching), and footprints must have been filled and buried by grainfall processes. Once covered by sand, the footprints would be protected from immediate erosion. Eventual deeper burial (>2 m) would have been required to acquire protection from subsequent bioturbation by plant roots and faunal burrowing activities. Trace fossils would still have been vulnerable to deep root bioturbation (roots sporadically penetrate to several meters below the dune surface into the vadose zone, as seen at several localities in the study area).

In some instances, the excellent preservation of footprints and wind ripples on palaeosurfaces testifies to burial soon after these features were formed. In general, the quality of footprint preservation at Still Bay depends on criteria such as the substrate consistency (moisture content and degree of compaction of dune sand), substrate slope and the time lapse between making and burial of the footprints.

The high detrital carbonate content of coastal dunes promotes rapid calcification by groundwaters in the vadose zone (Knox, 1977), which further enhances the preservation potential of footprints in this environment. Well calcified aeolianites at Kraal Bay, Langebaan Lagoon 130 km north of Cape Town, were dated by luminescence and radiocarbon to only ~10 ka (Roberts and Berger, 1997). Studies of thin sections of aeolianite calcified in the vadose zone revealed local bioclast dissolution and extensive secondary carbonate precipitation, typically as meniscate cements between grains (Knox, 1977).

5.3. Discussion

During the earlier historical period (19th century), some 400–600 individuals of the Cape elephant *Loxodonta africana africana* are inferred to have inhabited the narrow (~200 km long) forested coastal belt along the shores of the Indian Ocean (Skead, 1980). The species, which is similar in size and morphology to the savannah elephant *L. africana*, was hunted almost to extinction in the early 20th Century. A small group, the elusive 'Knysna elephants', occupied the temperate rainforest near the town of Knysna (Fig. 1), a few of which may still survive to the

present. It is therefore highly probable, based on both comparison of the footprints with modern African elephants and the information on historical elephant distributions, that the Still Bay footprints represent the extant Cape elephant *L. africana africana*. The abundant elephant footprints at Still Bay thus represent the southernmost occurrence of the African elephant recorded to date (34° 20′) i.e. ~5′ further south than the 'Knysna elephants'. Sea level at the time they were made was apparently below the present elevation, suggesting that they may have roamed even further south.

Trackways of extinct Late Tertiary proboscideans are well documented in east and north Africa (Leaky and Harris, 1987; Higgs et al., 2003). The tracks of *Loxodonta africana* reported from the lower !Khuiseb River silts in Namibia are historical in age (Kinahan et al., 1991). Thus the Last Interglacial elephant trackways reported here are, as far as we know, the only known fossil examples representing this species, and the only known Pleistocene footprints of proboscideans from Africa. A question that arises is the attraction to elephants of a seemingly inhospitable dunefield over an apparently considerable period. One possibility is the situation of the study area on a seasonal migration trail, examples of which in northern Botswana may have been in use for hundreds or even thousands of years (Stuart and Stuart, 1994). It seems probable though, that a difficult active dunefield terrain would have been avoided in a migration trail. Possibly, the elephants were lured to the area by a nearby source of water which may have been provided by an interdune wetland similar to Rietvlei, which exists in the area today (Fig. 2). Evidence for a contemporary interdune wetland was discussed in Section 3.3.

African elephants are adaptable to a range of environments, but generally require a high proportion of browse in their diet (Klein, 1983). Historically, elephants inhabiting the southern coast preferred the forested region (Fig. 1). Currently, the natural vegetation biome around Still Bay is dominated by the scrubland or '*fynbos*' of the Cape Flora and the nearest forested area is ~150 km eastwards around Knysna (Fig. 1). The presence of elephants around Still Bay during the Last Interglacial, seemingly in large numbers over a relatively prolonged period, may indicate more woodland and therefore a higher rainfall regime than at present. Such an inference is supported by evidence for a persistent high water table and strong groundwater flow inferred to be associated with palaeosol P1 and indications of a wetland environment at the base of the Still Bay Pleistocene aeolian succession (see Section 3.3). Furthermore, the preservation of numerous mammalian trackways witnesses frequent wetting of dune surfaces. The dominant southwesterly dune building winds (Fig. 7) testify to strong activity of cyclonic polar frontal systems.

Loxodonta africana was reported from the later Pleistocene Sea Harvest site (a carnivore lair bone accumulation) 130 km north of Cape Town (Klein, 1983). However, elephants do not occur in the Late Pleistocene fossil record along the southern Cape coast (Klein, 1983), so little is known about their distribution during this period. Evidence from palaeosol P1, consisting of rare (six) non-diagnostic stone artefacts and archaeological material from the nearby site of Blombos Cave (Fig. 1), witness a human presence around the time that elephants roamed the region. Furthermore, fossil human footprints have been reported in coastal aeolianites at Langebaan on the west coast and Nahoon on the southeast coast. Both occurrences were dated to the Last Interglacial (Roberts and Berger, 1997; Roberts, in press), further documenting a more widespread human presence at this time.

The elephants and humans would almost certainly have interacted. However, no proboscidian remains have been recovered from Blombos Cave or other Late Pleistocene cave deposits along the southern coast, but are recorded in the Holocene (Klein, 1983). Despite the evidence for human anatomical modernity in the region as early as the Last Interglacial, it would appear that the technological capability to exploit prey as formidable as elephants had yet to develop.

6. Conclusions

OSL and AAR analyses of the coastal aeolianite sequences at Still Bay reveal deposition primarily associated with MIS 5. AAR also demonstrated a notable re-working of bioclasts from older, pre-MIS 5 dunes into the Still Bay aeolianite succession. A pronounced depositional hiatus is recorded after ~90 ka, followed by Holocene dune accumulation from ~8 ka, coinciding with the fall in sea level associated with the Last Glacial and its rise approaching present levels during the early Holocene respectively. Dune sedimentation coincided with transgressive maxima and early regression i.e. proximity of a sandy beach was the overriding control (as at the present time). The dominant dune architectural element comprises large-scale, frequently convex-up, easterly orientated foresets consistent with parabolic dune migration under a westerly wind regime associated with polar frontal systems (as at the present time). Low-angle lamination is suggestive of interdunal sedimentation. Vertebrate ichnofossils are locally abundant in South African Pleistocene coastal aeolianites and preservation is excellent in some instances, supplementing data on faunal

distributions and thus contemporary climate and vegetation. The Still Bay elephants appear to have traversed the landscape in numbers, and are perhaps indicative of greater available arboreal browse vegetation and higher surface moisture conditions, an inference underpinned by evidence for wetland conditions in the aeolianite succession. Although evidence exists in the southern Cape for human anatomical modernity in the region as early as the Last Interglacial and despite the data presented here suggesting that the two species co-existed, available archaeological evidence does not indicate elephant predation.

Acknowledgements

This work was funded by the Leverhulme Trust research project grant (grant F/00 118/AF) awarded to MDB. The University of the Free State and Council for Geoscience are acknowledged for providing logistical support. We thank Mr Guy Gardner for permitting access to the sites and John Pether for mollusc identification.

References

Adams, R.W., 1983. General guide to the geological features of San Salvadore. In: Gerace, D.T. (Ed.), Field Guide to the Geology of San Salvadore, pp. 1–66.

Aitken, M., 1985. Thermoluminescence Dating. Academic Press, London.

Barwis, J.H., Tankard, A.J., 1983. Pleistocene shoreline deposition and sea-level history at Swartklip, South Africa. Journal of Sedimentary Petrology 53, 1281–1294.

Bateman, M.D., Catt, J.A., 1996. An absolute chronology for the raised beach deposits at Sewerby, East Yorkshire, U.K. Journal of Quaternary Science 11, 389–395.

Bateman, M.D., Holmes, P.J., Carr, A.S., Horton, B.P., Jaiswal, M.K., 2004. Aeolianite and barrier dune construction spanning the last two glacial-interglacial cycles from the southern Cape coast. South Africa Quaternary Science Reviews 23, 1681–1698.

Birkland, P., 1984. Soils and geomorphology. Oxford University Press, New York. 372 pp.

Bowman, G.M., 1979. Development of podzol soils in east Australian coastal and barrier sands. PhD Thesis, University of Sydney.

Brown, T., 1999. The Science and Art of Tracking. Berkley, New York. 154 pp.

Caputo, M.V., 1995. Sedimentary architecture of Pleistocene calcarenites, San Salvadore Island, Bahamas. Geological Society of America Special Paper 300, 63–76.

Carr, A.S., Thomas, D.S.G., Bateman, M.D., 2006a. Climatic and sea level controls on Late Quaternary aeolian activity on the Agulhas Plain, South Africa. Quaternary Research 65, 252–263.

Carr, A.S., Thomas, D.S.G., Bateman, M.D., Meadows, M.E., Chase, B., 2006b. Late Quaternary palaeoenvironments of the winter-rainfall zone of southern Africa: palynological and sedimentological evidence from the Agulhas Plain. Palaeogeography, Palaeoclimatology, Palaeoecology 239, 147–165.

Carr, A.S., Bateman, M.D., Holmes, P.J., 2007. Developing a 150 ka luminescence chronology for the coastal dunes of the southern Cape, South Africa. Quaternary Geochronology 2, 110–116.

Cohen, A.L., Tyson, P.D., 1995. Sea surface temperature fluctuations during the Holocene off the south coast of Africa: implications for terrestrial climate and rainfall. The Holocene, 5, 304–312.

Cowling, R.M., 1983. Phytochorology and vegetation history in the south-eastern Cape, South Africa. Journal of Biogeography 10, 393–419.

Deacon, H.J., 1995. Two Late Pleistocene–Holocene archaeological depositories from the southern Cape, South Africa. South African Archaeological Bulletin 50, 121–131.

Deacon, H.J., Deacon, J., 1999. Human Beginnings in South Africa. David Phillip Publishers, Cape Town. 214 pp.

Dingle, R.V., Rogers, J., 1972. Effects of sea-level changes on the Pleistocene palaeoecology of the Agulhas bank. Palaeoecology of Africa 6, 55–58.

Duller, G.A.T., 2003. Distinguishing quartz and feldspar in single grain luminescence measurements. Radiation Measurements 37, 161–165.

Fryberger, S.G., Ahlbrandt, T.S., Andrews, S., 1979. Origin, sedimentary features, and significance of low-angle aeolian "sand sheet" deposits, Great Sand Dunes National Monument and vicinity, Colorado. Journal of Sedimentary Petrology 49, 733–746.

Galbraith, R.F., Roberts, R.G., Laslett, G.M., Yoshida, H., Olley, J.M., 1999. Optical dating of single and multiple grains of quartz from Jinmium rock shelter, northern Australia. Part I: experimental design and statistical models. Archaeometry 41, 339–364.

Henshilwood, C.S., Sealy, J.C., Yates, R., Cruz-Uribe, K., Goldberg, P., Grine, F.E., Klein, R.G., Poggenpoel, C., Van Niekerk, K., Watts, I., 2001. Blombos Cave, southern Cape, South Africa: preliminary report on the 1992–1999 excavations of the middle stone age levels. Journal of Archaeological Science, 28, 421–448.

Henshilwood, C.S., d'Errico, F., Yates, R., Jacobs, Z., Tribolo, C., Duller, G.A.T., Mercier, N., Sealy, J.C., Vallada, H., Watts, I., Wintle, A.G., 2002. Emergence of modern human behavior: Middle Stone Age engravings from South Africa. Science 295, 1278–1280.

Higgs, W., Kirkham, A., Evans, G., Hull, D., 2003. A Late Miocene Proboscidean Trackway from Mleisa, United Arab Emirates. Tribulus Journal of the Emirates Natural History Group 13.2, 3–8.

Hunter, R.E., 1977. Basic types of stratification in small aeolian dunes. Sedimentology 24, 361–387.

Hunter, R.E., 1981. Stratification Styles in Aeolian Sandstones: Some Pennsylvanian to Jurassic Examples from the Western Interior U.S.A. SEPM Special Publication, vol. 31, pp. 315–329.

Hutchinson, J.R., Famini, D., Lair, R., Krams, R., 2003. Are fast-moving elephants really running? Nature 422, 493–494.

Illenberger, W.K., 1996. The geomorphic evolution of the Wilderness dune cordons, South Africa. Quaternary International 33, 11–20.

Irving, S.J., 1998. Late Quaternary Palaeoenvironments at Vankervelsvlei, near Kynsna, South Africa.Unpublished MSc thesis, University of Cape Town.

Jacobs, Z., Wintle, A.G., Duller, G.A.T., 2003. Optical dating of dune sand from Blombos Cave, South Africa: I-multiple grain data. Journal of Human Evolution 44, 599–612.

Kaufman, D.S., Manley, W.F., 1998. A new procedure for determining D/L amino acid ratios in fossils using reverse phase liquid chromatography. Quaternary Geochronology (Quaternary Science Reviews) 17, 987–1000.

Kinahan, J., Pallett, J., Vogel, J., Ward, J., Lindeque, M., 1991. The occurrence and dating of elephant tracks in the silt deposits of the Lower !Khuiseb River. Cimbasia, 13, 37–43.

Klappa, C.F., 1980. Rhizoliths in terrestrial carbonates: classification, recognition, genesis and significance. Sedimentology 27, 613–629.
Klein, R.G., 1983. Palaeoenvironmental implications of Quaternary large mammals in the fynbos region. In: Deacon, H.J., Hendey, Q.B., Lambrechts, J.J.N. (Eds.), Fynbos Palaeoecology: A Preliminary Synthesis, pp. 116–133.
Knox, G.J., 1977. Caliche profile formation, Saldanha Bay (South Africa). Sedimentology 24, 657–674.
Kraus, M.J., 1999. Paleosols in clastic sedimentary rocks: their geologic applications. Earth Science Review 47, 41–70.
Kruger, A.C., 2004. Climate of South Africa: Climate Regions. WS 45. South African Weather Service, Pretoria, South Africa. 19 pp.
Leakey, M.D., Harris, J.M., 1987. Laetoli, A Pliocene Site in Northern Tanzania. Oxford University Press, pp. 451–489.
Le Roux, F.G., 1989. Lithostratigraphy of the Nahoon Formation (Algoa Group). South African Committee for Stratigraphy, Lithostratigraphic Series Number 9, Department of Mineral and Energy Affairs. 14 pp.
Malan, J.A., 1989. Lithostratigraphy of the Waenhuiskrans Formation (Bredasdorp Group). South African Committee for Stratigraphy (SACS), Lithostratigraphic Series Number 8, Department of Mineral and Energy Affairs.
Malan, J.A., 1990. The stratigraphy and sedimentology of the Bredasdorp Group, Southern Cape Province. Unpublished M. Sc. Thesis, University of Cape Town, 197 pp.
Marsh, R.E., Prestwich, W.V., Rink, W.J., Brennan, B.J., 2002. Monte Carlo determinations of the beta dose rate to tooth enamel. Radiation Measurements 35, 609–616.
Martin, A.R.H., 1959. The stratigraphy and history of Groenvlei, a South African coastal fen. Australian Journal of Botany 7, 142–167.
Martin, A.R.H., 1962. Evidence relating to the Quaternary history of the Wilderness lakes. Transactions of the Geological Society of South Africa 65, 19–45.
McKee, E.D., 1944. Tracks that go uphill. Plateau 16, 61–72.
McKee, E.D., 1966. Structures of dunes at Whitesands National Monument, New Mexico (and a comparison with structures from other selected areas). Sedimentology 7, 1–69.
Murray, A.S., Wintle, A.G., 2000. Luminescence dating of quartz using an improved single-aliquot regenerative-dose protocol. Radiation Measurements 32, 57–73.
Murray, A.S., Wintle, A.G., 2003. The single aliquot regenerative dose protocol: potential for improvements in reliability. Radiation Measurements 37, 377–381.
Murray-Wallace, C.V., Brooke, B.P., Cann, J.H., Belperio, A.P., Bourman, R.P., 2001. Whole-rock aminostratigraphy of the Coorong Coastal Plain, South Australia: towards a 1 million year record of sea-level highstands. Journal of the Geological Society, London 158, 111–124.
Olley, J.M., Murray, A.S., Roberts, R.G., 1996. The effects of disequilibria in the uranium and thorium decay chains on burial dose rates in fluvial sediments. Quaternary Science Reviews 15, 751–760.
Pearson, O.M., Grine, F.E., 1997. Re-analysis of the hominid radii from Cave of Hearths and Klasies River Mouth, South Africa. Journal of Human Evolution 32, 577–592.
Prescott, J.R., Hutton, J.T., 1994. Cosmic ray contributions to dose rates for luminescence and ESR dating: large depths and long-term variations. Radiation Measurements, 23, 497–500.
Retallack, G.J., 2001. Soils of the Past, 2nd ed. Blackwell Science, New York.
Rightmire, G.P., Deacon, H.J., 1991. Comparative studies of Late Pleistocene human remains from Klasies River Mouth, South Africa. Journal of Human Evolution 20, 131–156.
Roberts, D.L., 2003. Vertebrate trackways in Pleistocene coastal calcareous aeolianites South Africa. Abstract, XVl Inqua Congess, Reno, Nevada, p. 96.
Roberts, D.L., Berger, L., 1997. Last interglacial (c.117 kyr) human footprints South Africa. South African Journal of Science 93, 349–350.
Roberts, D.L., Brink, J., 2002. Dating and correlation of Neogene coastal deposits in the Western Cape, South Africa: implications for Neotectonism. South African Journal of Geology 105, 337–352.
Roberts, D.L., in press. Last interglacial hominid and associated vertebrate fossil trackways in coastal aeolianites, South Africa. Ichnos, Special Issue: Volume Hominid Ichnology.
Skead, C.J., 1980. Historical Mammal Occurrence in the Cape Province, vol 1: The Western and Northern Cape. Provincial Administration of the Cape of Good Hope.
South African Weather Bureau, 1986. Climate of South Africa. Publication WB, vol. 40. 474 pp.
Stuart, C., Stuart, T., 1994. A Field Guide to the Tracks and Signs of East and South African Mammals. Southern Book Publishers, Cape Town.
Sweet, M.L., 1992. Lee-face air flow, surface processes, and stratification types: their significance for refining the use of cross-strata as paleocurrent indicators. Geological Society Bulletin 104, 1528–1538.
Thompson, C.H., 1981. Podzol chronosequences on coastal dunes of eastern Australia. Nature 291, 59–61.
Tinley, K.L., 1985. Coastal dunes of South Africa. South African National Scientific Programmes report no. 109. Foundation for Research Development, Council for Scientific and Industrial Research, Pretoria. 300 pp.
Tyson, P.D., 1999. Late-Quaternary and Holocene palaeoclimates of southern Africa: a synthesis. South African Journal of Geology 102, 335–349.
Walker, N.D., 1990. Links between South African summer rainfall and temperature variability in the Agulhas and Benguela Current systems. Journal of Geophysical Research, 95, 3297–3319.
Western, D., Moss, C., Georgiadis, N., 1983. Age estimation and population age structure of elephants from footprint dimensions. Journal of Wildlife Management 47, 1192–1197.